



The influence of land use and management on the behaviour and persistence of soil organic carbon in a subtropical Ferralsol

Laura Hondroudakis¹, Peter M. Kopittke¹, Ram C. Dalal¹, Meghan Barnard¹, and Zhe H. Weng^{1,2}

¹School of Agriculture and Food Sustainability, The University of Queensland,
St Lucia, Queensland 4072, Australia

²School of Agriculture, Food, and Wine, Urrbrae, The University of Adelaide,
South Australia 5064, Australia

Correspondence: Peter M. Kopittke (p.kopittke@uq.edu.au)

Received: 11 December 2023 – Discussion started: 22 December 2023

Revised: 4 May 2024 – Accepted: 17 May 2024 – Published: 4 July 2024

Abstract. A substantial carbon (C) debt has been accrued due to long-term cropping for global food production emitting carbon dioxide from soil. However, the factors regulating the persistence of soil organic C (SOC) remain unclear, with this hindering our ability to develop effective land management strategies to sequester organic C in soil. Using a Ferralsol from semi-arid subtropical Australia, alteration of bulk C contents and fractions due to long-term land use change (up to 72 years) was examined with a focus on understanding whether SOC lost due to cropping could be restored by subsequent conversion back to pasture or plantation. It was found that use of soil from cropping for 72 years resulted in the loss of > 70 % of both C and N contents. Although conversion of cropped soil to pasture or plantation for up to 39 years resulted in an increase in both C and N, the C contents of all soil fractions were not restored to the original values observed under remnant vegetation. The loss of C with cropping was most pronounced from the particulate organic matter fraction, whilst in contrast, the portion of the C that bound strongly to the soil mineral particles (i.e. the mineral-associated fraction) was most resilient. Indeed, aliphatic C was enriched in the fine fraction of mineral-associated organic matter (< 53 µm). Our findings were further confirmed using Synchrotron-based micro-spectroscopic analyses of intact microaggregates, which highlighted that binding of C to soil mineral particles is critical to SOC persistence in disturbed soil. The results of the present study extend our conceptual understanding of C dynamics and behaviour at the fine scale where C is stabilized and accrued, but it is clear that restoring C in soils in semi-arid landscapes of subtropical regions poses a challenge.

1 Introduction

The release of greenhouse gas (GHG) emissions from anthropogenic sources has increased rapidly over the last few decades despite rigorous international efforts to reduce emissions. Globally, soil organic carbon (SOC) stocks have been reduced by 20 %–60 % with land use change to long-term cropping (Kopittke et al., 2017), with land use change having released an estimated 116 Pg of carbon (C) to the atmosphere (Sanderman et al., 2017). However, this current C debt also corresponds to an opportunity to sequester atmospheric

C (Sykes et al., 2020). Soils are second only to the oceans in their C storage size, and the amount of C stored in the atmosphere (875 GtC) and vegetation (450 GtC) combined is less than that in soils (1700 GtC outside of permafrost regions) (Friedlingstein et al., 2022).

SOC positively influences soil water, structure, health, and plant productivity, and protecting and building SOC is essential to climate change mitigation (Lehmann et al., 2020a; Oldfield et al., 2019). To optimize SOC sequestration, the complex behaviour of C in soils and the factors which control its dynamics need to be understood. Lehmann et al. (2020b)

proposed that functional complexity from the interactions between molecular diversity (i.e. C forms), spatial heterogeneity (i.e. distribution of C forms), and temporal variability in the soil system regulates the persistence of SOC. The first of these factors, molecular diversity, is important because a higher diversity of molecules will increase the metabolic cost for micro-organisms past a certain threshold as large molecules are more difficult to assimilate. The second of these factors, spatial heterogeneity, refers to the spatial distribution of C forms and the associated likelihood of decomposers to access this SOC due to adsorption of SOC to mineral surfaces and metal ions and occlusion within aggregates. The final factor, temporal variability, also influences the persistence of SOC as changes in conditions such as nutrients, temperature, and moisture impact the activities of microbes, resulting in changes to decomposition. How these three factors, molecular diversity, spatial heterogeneity, and temporal variability, interact and the influence that this and land use change have on SOC persistence are only poorly understood (Lehmann et al., 2020b). This is especially true in tropical and subtropical soil, with many previous studies having been conducted in temperate systems such as in Europe and North America. Furthermore, there is uncertainty regarding the composition and formation of aggregates and mineral-associated SOC and subsequently how these can be influenced by land management practices (Angst et al., 2021).

The objective of the present study was to improve our understanding of the impact of long-term land use change on SOC and the underlying factors regulating its persistence by examining both the molecular diversity and spatial heterogeneity of SOC. Specifically, the aims were threefold: to investigate the impacts of land use change on bulk C contents and pools, the shift of C forms, and the fine-scale distribution of C forms. A Ferralsol from subtropical southeast Queensland, Australia, was used, and four land uses were compared: (i) undisturbed soil (remnant vegetation), (ii) a cropped soil, (iii) pasture, and (iv) plantation. First, the alteration of bulk C contents due to land use change was quantified. Next, the properties of this SOC were compared between land uses, with this providing critical information on the properties regulating SOC persistence – for this, changes in microbial respiration and fractionation were examined. In addition, Synchrotron-based soft X-ray spectroscopy (SXR) was used to non-destructively identify the C forms within each land use. Finally, to improve our understanding regarding the fine-scale distribution of C, the lateral distribution of C forms at microscale was compared between land uses using Synchrotron-based infrared microspectroscopy (IRM) analyses. The information obtained from these analyses contributes to the emerging body of evidence that soil functional complexity substantially influences C turnover and persistence.

2 Materials and methods

2.1 Soil collection and study site

Soil samples were collected from Kingaroy in south-east Queensland, Australia (26.7° S, 151.8° E). Using the World Reference Base, this soil is classed as a Ferralsol (being a Ferrosol in the Australian Soil Classification) and has developed on basalt flows that have been intensely weathered. The site is in a lower rainfall environment (676 mm yr⁻¹) and has a slope of < 5%. Soil was collected from four land uses which were all within 700 m of one another (Fig. 1): (a) remnant vegetation, (b) land which was converted from remnant vegetation to cropping (peanut–maize cultivation) for 33 years and then converted to pasture for 18 years before being converted to plantation (*Corymbia citriodora*, subsp. *variegata*) for the last 21 years (“plantation”), (c) land which was converted from remnant vegetation and has been used for cropping (peanut–maize cultivation) for the last 72 years (“cropped”), and (d) land which was converted from remnant vegetation to cropping (peanut–sorghum–maize cultivation) for 33 years and then grazed pasture for the last 39 years (“pasture”) (Table S1 and Fig. S1 in the Supplement; Zhang et al., 2020). Within each land use, five replicate samples were taken at random points within 10 m of each other, with soil collected to a depth of 0–10 cm. As noted by Zhang et al. (2020) for this experimental system, this depth of sampling (0–10 cm) corresponds to the depth of soil disturbance by tillage, with the cropped soils having been tilled by conventional tillage practices since their conversion from native vegetation. Although the cropped soils have had fertilizer applied, no fertilizers have been applied to the pasture or plantation soils (Table S1). No lime has been applied. Further information on the soil properties is provided by Zhang et al. (2020).

2.2 Bulk analyses

All samples were air-dried (~ 40 °C) and sieved to < 2 mm before further analyses were conducted. The electrical conductivity (EC) and pH were measured using a 1 : 5 soil/water suspension at 25 °C as described in Rayment and Lyons (2011). The total organic C and N were determined through Dumas high-temperature combustion with no soil pre-treatment (Rayment and Lyons, 2011) since no carbonate-C was present (soil pH ≤ 5.5). Each sample was finely ground (< 0.5 mm) using a ceramic pestle and mortar, and 1.00 g was weighed into combustion boats. The concentrations of total organic C and N were measured using a carbon–nitrogen analyser (LECO Trumac CN analyser, MI).

Exchangeable cations (Al³⁺, Ca²⁺, Mg²⁺, Na⁺, K⁺) were determined by extraction in 1 M NH₄Cl at pH 7 without the pre-treatment for soluble salts as outlined in method 15A1 in Rayment and Lyons (2011). The extracts were then analysed using inductively coupled plasma optical emission spec-

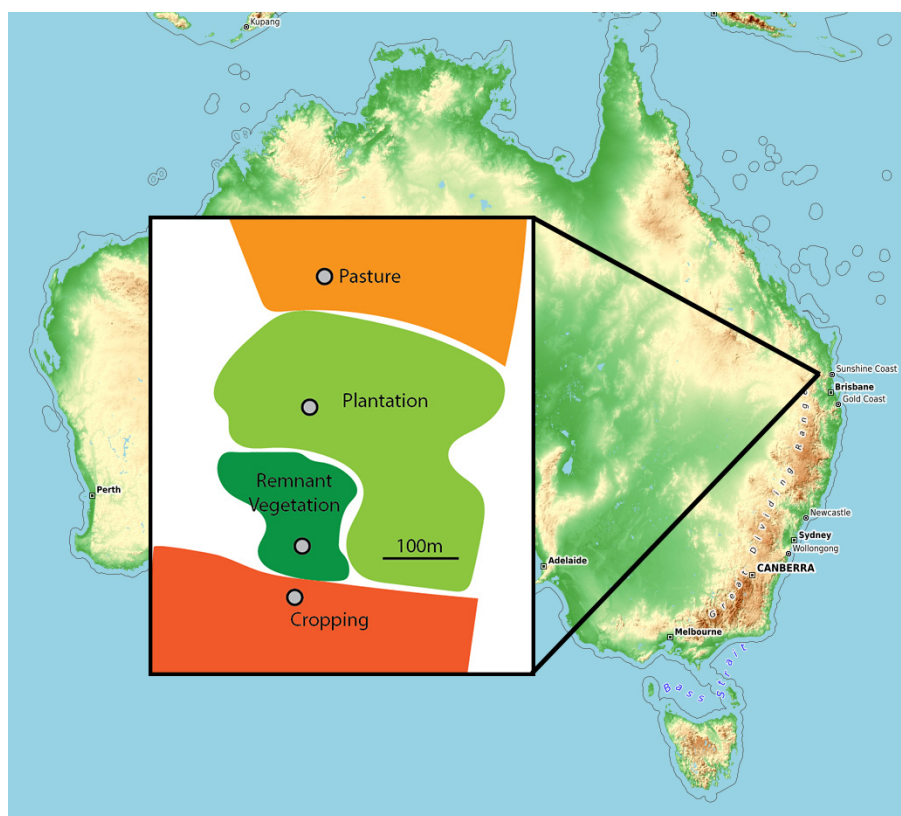


Figure 1. Schematic diagram of sampling design with sample locations and land use pattern illustrated. Image from Getlost Maps.

troscopy (ICP-OES). The effective cation exchange capacity (ECEC) was determined by summing the exchangeable cations. The potentially plant-available P concentration was determined by extraction with bicarbonate (Colwell-P) and analysis in a SEAL AQ400 discrete analyser as described in method 9B1 of Rayment and Lyons (2011).

2.3 Microbial respiration

The susceptibility of the SOC to microbial decomposition was determined by measuring microbial respiration (by CO_2 release) in a 15 d incubation experiment by a method adapted from Niaz et al. (2022). There was a total of 20 experimental units, comprising five replicates for each of the four land uses. For each of the experimental units, 25 g of field soil was added to 250 mL jars and then wetted to 80 % field capacity. The soil water content at field capacity (-0.1 bar) was determined by wetting soil to saturation and then allowing it to drain for 24 h. To maintain 80 % field capacity throughout the incubation period, the jars were stored (with lids removed) in a humid environment at 25 °C, and additional deionized water was added to the jars throughout the incubation experiment to keep a consistent weight representing 80 % field capacity (± 0.2 mL). Four blanks were included to measure the background CO_2 . The jars were covered with lids having two holes that had Luer locks inserted into these holes and ar-

ranged in a completely randomized design. The jar lids were closed (not allowing any air transfer) for 2 h prior to measurement. After 2 h, each jar was connected via rubber tubing to a CO_2 analyser (WMA-4 CO_2 analyser, John Morris USA) to record the concentration of CO_2 . The first 3 d was allowed for equilibration, with data recorded every day thereafter for the first 5 d, and then at 2 d interval after this. The measurements were converted to $\text{mg CO}_2\text{-C kg}^{-1}\text{ d}^{-1}$ from the volume of CO_2 in the headspace of the respiration jars. Cumulative CO_2 produced during the incubation experiment was calculated by summation of the recorded CO_2 over each day for the incubation period.

2.4 Density fractionation

The density fractionation method was adapted from Kölbl and Kögel-Knabner (2004) and Steffens et al. (2009) (Fig. S2). Briefly, 20 g bulk soil was added to a 200 mL sodium polytungstate (1.8 g cm^{-3}) solution, and the floating free particulate organic matter (POM) (“fPOM”) was collected by aspiration. The soil was not shaken within the sodium polytungstate (SPT) to minimize any disturbance. To separate the aggregate-occluded POM (“oPOM”) from the remaining sample, the soil was subjected to sonification in two waves of 200 J mL^{-1} (total of 400 J mL^{-1}) and then centrifuged. The use of 400 J mL^{-1} for sonication was

based upon a preliminary experiment to maximize recovery of POM at the lowest possible energy input, with this value being in accordance with previous studies for reactive soils (Asano and Wagai, 2014; Spielvogel et al., 2007). The floating oPOM was collected by aspiration. The fPOM was manually washed, and the oPOM was washed using pressure filtration (operated at 5 bar), with ultrapure Milli-Q water until the filtrate for both fractions was $EC < 5 \mu S cm^{-1}$. The remaining mineral-associated organic matter (MAOM) fraction was washed using pressure filtration to an $EC < 50 \mu S cm^{-1}$ and then sieved under gravity using a $53 \mu m$ steel sieve to separate the fine-fraction MAOM ($> 53 \mu m$) from the coarse-fraction MAOM ($< 53 \mu m$). The fPOM and oPOM were freeze-dried, and the MAOM fractions were oven-dried at $50^\circ C$. The samples were finely ground for total C and N analysis by isotope ratio mass spectrometry (IRMS). The results for the C contents of each fraction were termed the “fPOC” (free particulate organic C), “oPOC” (aggregate-occluded organic C), “coarse-fraction MAOC” (organic C associated with the coarse mineral fraction ($> 53 \mu m$)), and the “fine-fraction MAOC” (organic C associated with the fine mineral fraction ($< 53 \mu m$)). Similarly for N, the results giving the N contents of each fraction were termed the “fPON”, “oPON”, “coarse-fraction MAON”, and “fine-fraction MAON”.

2.5 Synchrotron-based near-edge X-ray absorption fine-structure spectroscopy

All samples were air-dried ($\sim 40^\circ C$), sieved to $< 2 mm$, and ground to a fine powder using a mortar and pestle. One composite sample per land use was generated by combining each of the five replicates. The composites were attached to a plate of stainless steel using double-sided C tape. Samples were analysed at the SXR beamline at the Australian Synchrotron (Clayton, Australia). The partial electron yield method was used to collect near-edge X-ray absorption fine-structure (NEXAFS) spectroscopy C K-edge spectra. To counter charging effects of soil minerals, a flood gun was used with partial electron yield. A calculated energy resolution of $0.05 eV$ at a $280 eV$ photon energy was obtained by setting the beamline grating exit slits to $20 \mu m$. The spectra were acquired at an angle of 55° to the beam and over a photon energy range of 275 to $325 eV$, at a $0.1 eV$ step size. For baseline correction, the pre-edge energy range was 270 and $275 eV$, and the post-edge energy range was 325 and $340 eV$. The energy of the beamline (270 – $340 eV$) was calibrated using a graphite standard. Concurrently, the sample NEXAFS and incident intensity (I_0) spectra were collected (Weng et al., 2017).

A photodiode measurement obtained in the ultra-high-vacuum (UHV) analytical chamber and the I_0 were used to normalize the spectra. The double-normalization method, as described by Stöhr (2013), was utilized to carry out the normalization. Data were normalized using the Igor software (v8.04.2) with a pre- and post-edge linear subtraction.

Double-normalized spectra were deconvoluted using Athena 0.9.26 (Ravel and Newville, 2005). Deconvolution and curve fitting were conducted as described by Prietzel et al. (2018) using the PeakFit procedure in Athena (Fig. S3). An arctan function (energy: $290 eV$, fixed height of 1) was used to represent the edge step. Six Gaussian peaks were then fitted for the six major C electron transition groups, (1) 284.7 , (2) 285.5 , (3) 287.3 , (4) 288.2 , (5) 289.0 , and (6) $289.8 eV$, with fixed widths of $0.4 eV$. Two additional Gaussian peaks were set at 292 and $294 eV$ (width $1.5 eV$), representing broad additional $1s \rightarrow \sigma^*$ transitions of saturated single covalent bonds and direct inner-shell ionization (Prietzel et al., 2018). The contributions of the various C functional groups were calculated as the area under the Gaussian peaks divided by the sum of these areas.

2.6 Synchrotron-based infrared microspectroscopy

All samples were air-dried ($\sim 40^\circ C$) and sieved to $< 2 mm$. One composite sample per land use was generated by combining each of the five replicates. Typical free microaggregates (ca. 20 – 30) of 53 – $250 \mu m$ were humidified and then frozen at $-20^\circ C$. A diamond knife was used to cryo-ultramicrotome semi-thin sections (ca. $200 nm$ thickness) of microaggregates without embedding media. Thin soil sections were transferred to CaF_2 windows ($13 mm$ diameter, $0.5 mm$ thickness). The samples were analysed at the Australian Synchrotron using the IRM beamline in transmission mode. A detection aperture to sample an area of $5 \mu m \times 5 \mu m$ was selected. To produce the maps, 32 co-added scans ($4 cm^{-1}$ resolution) were taken ($2.5 \mu m$ step size over ca. $50 \mu m \times 50 \mu m$).

The software OPUS 8.7.31 (Bruker Optik GmbH, Germany) was used to process spectral maps. Map profiles were created for specific absorbances which coincide with the peaks of relevant C functional groups and O–H groups of clay minerals. A map profile for absorbance at $3630 cm^{-1}$ was created as this peak corresponds with the stretching vibrations of O–H clay minerals. Similarly, the peak at $1035 cm^{-1}$ corresponds to the C–O stretching vibration of polysaccharide C, the C=C stretching of aromatic C (or N–H deformations) corresponds to a peak at $1600 cm^{-1}$, and the peak at $2920 cm^{-1}$ corresponds to the C–H stretching of aliphatic biopolymers. On either side of the absorbance peaks (3550 – $3740 cm^{-1}$ (O–H groups of clays), 950 – $1170 cm^{-1}$ (polysaccharide C), 1500 – $1750 cm^{-1}$ (aromatic C), 2800 – $3000 cm^{-1}$ (aliphatic C)) appropriate baseline points were selected so that the integrated area under each absorbance peak could be applied to the map.

2.7 Statistical analyses

Repeated measures analyses were performed for all data using a linear mixed model framework (REML) using the Genstat software (Version 23.1.0.651). Each analysis for organic

C content, total organic C per fraction, and deconvolution of NEXAFS consisted of a fixed model of land use, fraction, and their associated interactions and a random effect of the replicate (Fang et al., 2022). Tukey's post hoc testing was used to identify significant differences based on the REML mixed-effects model ($p < 0.05$). To determine the significance level, a one-way analysis of variance (ANOVA) was completed with land use as a factor, for the bulk soil properties, respiration rate and cumulative respiration at each time point to determine if there were any significant differences between the sites using R version 4.2.1 (R Core Team, 2021). The ANOVA was checked for the normal distribution of residuals and homogeneity of variances (Fig. S4). Where the ANOVA identified a significant difference in land use ($p < 0.05$), the least significant difference (LSD) (95 % confidence level for each comparison) was calculated to determine which land uses differed significantly from one another. A two-way ANOVA was completed with fraction and land use as factors for the density fractionation data. The data frame was then split into each fraction, where one-way ANOVA was used to identify significant differences between land uses followed by calculating the LSD to compare the means of each land use.

For the Synchrotron-based IRM, correlations between the polysaccharide C, aromatic C, or aliphatic C and the amount of clay were examined using simple linear regression. The relative strength of associations was indicated by the regression gradients, and the residual variability affiliated with the associations was indicated by the R^2 coefficients. It is important to note that both the Synchrotron-based IRM and NEXAFS techniques, as performed in the present study, are considered qualitative methods for characterizing C forms and distribution.

3 Results

3.1 Bulk C contents and pools

There was a significant difference in the pH (1 : 5 suspension) between the various land uses ($p = 0.026$), with the plantation soil having a significantly lower pH (5.0) compared with the pasture soil (5.5, Table 1). For EC (1 : 5 suspension), no significant differences were found between the land uses, with an average value of 0.11 dS m^{-1} (Table 1). There were substantial differences in the ECEC values ($p < 0.01$), which was significantly lower for the cropped soil ($3.0 \text{ cmol}_c \text{ kg}^{-1}$) than the other land uses ($7.5 \text{ cmol}_c \text{ kg}^{-1}$; Table 1). Furthermore, there were significant differences in the Colwell-P concentration ($p < 0.01$), with the crop (58 mg kg^{-1}) and pasture soils (51 mg kg^{-1}) both having higher extractable P than the remnant vegetation (18 mg kg^{-1}) and plantation (19 mg kg^{-1} ; Table 1).

Notably, the total SOC content differed between land uses ($p < 0.01$) and decreased in the order of remnant vegetation (81 g kg^{-1}) \approx plantation (63 g kg^{-1}) $>$ pasture (38 g kg^{-1})

\approx cropped (18 g kg^{-1}) (Table 1). Hence, the conversion of remnant vegetation to cropped resulted in a 78 % decrease in SOC in the surface 0–10 cm. Changes in total N were similar to those described above for C ($p < 0.01$), being highest in the remnant vegetation soil (5.9 g kg^{-1}) and lowest in the cropped soil (1.6 g kg^{-1}). The C : N ratio varied from 12 in the cropped soil to 14 in the remnant vegetation, 12 in the pasture, and 16 in the plantation (Table 1).

3.2 Microbial respiration

The cropped soil had a significantly lower microbial respiration rate ($0.0069 \text{ mg CO}_2\text{-C g}^{-1} \text{ d}^{-1}$) compared to the pasture, remnant vegetation, and plantation soils ($0.020 \text{ mg CO}_2\text{-C g}^{-1} \text{ d}^{-1}$; Fig. 2a). When examined as cumulative respiration over the 15 d experimental period, the cropped soil had a significantly lower cumulative respiration ($0.13 \text{ mg CO}_2\text{-C g}^{-1}$) compared to all other land uses by the final day of incubation ($0.29 \text{ mg CO}_2\text{-C g}^{-1}$; Fig. 2b).

3.3 Density fractionation

In the remnant vegetation soil, the fPOC fraction (22.3 mg C g^{-1} of bulk soil) and fine-fraction MAOC (19.8 mg C g^{-1} of bulk soil) were the two largest fractions, with the coarse-fraction MAOC (7.59 mg C g^{-1} of bulk soil) and the oPOC (9.29 mg g^{-1} of bulk soil) being considerably smaller (Fig. 3a). Indeed, for the remnant vegetation, the fPOC and the fine-fraction MAOC accounted for 71 % of the total bulk organic C (Fig. 3b). Similarly for N, the fine-fraction MAON (2.14 mg N g^{-1} of bulk soil) and fPON (1.58 mg N g^{-1} of bulk soil) were the largest pools for the remnant vegetation soil (Fig. S5).

The decrease in total organic C observed for all three other land uses compared to the remnant vegetation soil (Table 1) was associated with a decrease in the absolute contribution of all four fractions for the cropped soil and pasture (fPOC, oPOC, the coarse-fraction MAOC, and fine-fraction MAOC) and all fractions except the fPOC for the plantation (Fig. 3a). However, the relative contribution of each fraction to the total organic C varied with land use change. For the conversion of remnant vegetation to cropped, the fPOC fraction was the most labile (least stable) with land use change, with its relative contribution to the total SOC decreasing from 37 % in the remnant vegetation soil to only 17 % in the cropped soil (Fig. 3b). In contrast, the fine-fraction MAOC was the most stable fraction, with its relative contribution to total SOC increasing from 37 % in the remnant vegetation soil to 55 % in the cropped soil. In addition, the loss in fPON content was even greater than observed for fPOC with a decrease from 1.6 mg N g^{-1} of bulk soil in the remnant vegetation to only 0.12 mg N g^{-1} of bulk soil in the cropped soil, a decrease of 92 % (Fig. S5), with cropped soil also having a higher C : N ratio (20.5) than remnant vegetation (14.1) (Table S2).

Table 1. Mean values (standard errors in parentheses) of the bulk soil from each land use. Lower-case letters reflect least significant differences ($P < 0.05$) for pH, electrical conductivity (EC), effective cation exchange capacity (ECEC), phosphorus, total organic carbon, and total N. Values are the average of five replicates.

Land use	pH (1 : 5 water)	EC (dS m ⁻¹) (1 : 5 water)	ECEC (cmol ₍₊₎ kg ⁻¹)	Colwell P (mg kg ⁻¹)	Total organic C (g kg ⁻¹)	Total N (g kg ⁻¹)	C : N ratio
Remnant vegetation	5.2 ^{ab} (0.13)	0.13 (0.19)	8.7 (0.80) ^a	18 ^b (1.2)	81 ^a (13)	5.9 ^a (0.74)	14 (0.50)
Pasture	5.5 ^a (0.09)	0.081 (0.01)	6.3 (0.53) ^b	51 ^a (6.5)	38 ^b (2.0)	3.1 ^b (0.08)	12 (0.41)
Plantation	5.0 ^b (0.07)	0.12 (0.02)	7.5 (0.87) ^{ab}	19 ^b (3.7)	63 ^a (8.6)	3.9 ^b (0.46)	16 (0.33)
Cropped	5.2 ^{ab} (0.09)	0.10 (0.014)	3.0 (0.29) ^c	58 ^a (6.0)	18 ^b (1.9)	1.6 ^c (0.13)	12 (0.40)

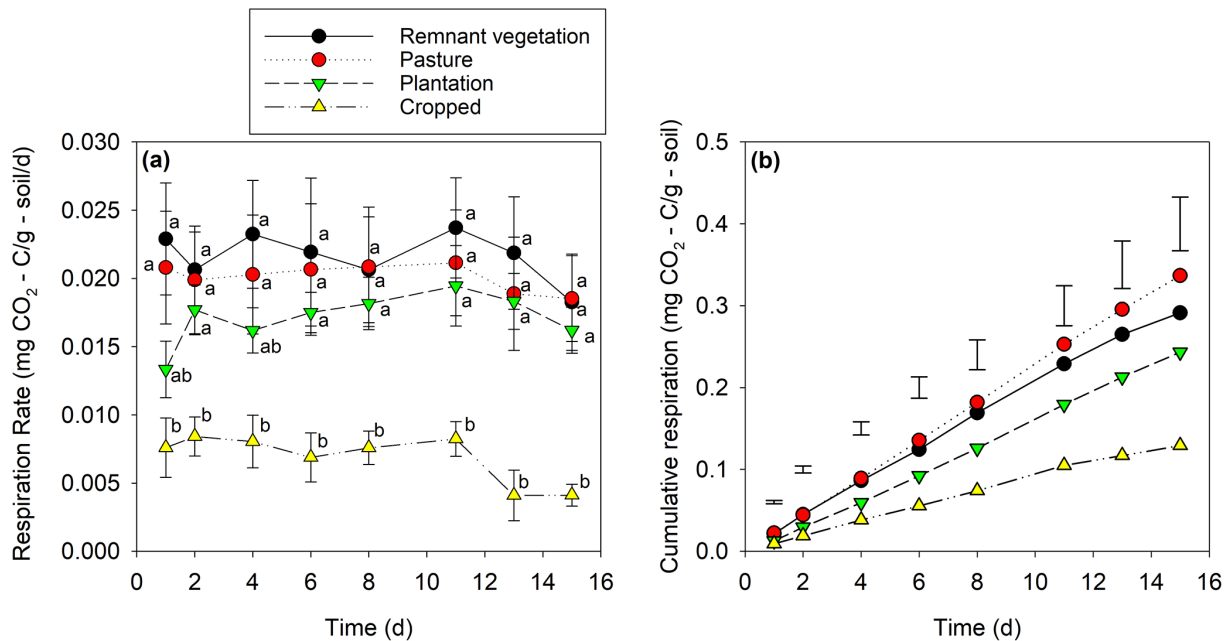


Figure 2. (a) Mean (with standard error) respiration rates of soil for four land uses. Letters indicate the least significant difference ($P < 0.05$) between the land uses at each time. (b) Cumulative respiration for four land uses across a 15 d incubation period. Each point represents the mean of five replicates. Error bars indicate least significant differences ($P < 0.05$) between land uses at each time.

Restoration of cropped land to pasture significantly increased the absolute C content of all fractions except for the fPOC (Fig. 3a). However, these increases in the oPOC and MAOC fractions were not enough to restore SOC to the original values observed under remnant vegetation (Fig. 3a). The fine-fraction MAOC pool was still the largest fraction for the pasture soil, accounting for 58 % of the total C, with a similar value observed for the cropped soil (55 %) (Fig. 3b). A similar pattern was observed for organic N in the various fractions as described for organic C (Fig. S5).

Finally, restoration of cropped soil to plantation resulted in a significant increase in both organic C and N content of all fractions (Figs. 3a and S5). However, despite the conversion of cropping to pasture increasing C and N, contents still remained lower for all fractions compared to the remnant vegetation, with the exception being for the fPOC fraction for the plantation soil (18.1 mg C g⁻¹ of bulk soil) which was

not significantly different from the remnant vegetation soil (22.3 mg C g⁻¹ of bulk soil).

3.4 Land use impacts on C forms: Synchrotron-based near-edge X-ray absorption fine-structure spectroscopy

To examine the effect of long-term land use change on the forms of organic C and N within the soil, Synchrotron-based NEXAFS was used. The C K-edge spectra had clear peaks for all land uses at 284.7 eV indicating the presence of quinones (C=O), 285.5 eV indicating aromatic C and double-bonded alkyl C (C=C), 287.3 eV indicating aliphatic C and phenolic C–OH, (aromatic C with side chain N-substituted aromatic C), 288.2 eV indicating aliphatic C (alkyl C, C–H), 289.0 eV indicating carboxyl C–OOH functional groups, and 289.8 eV indicating O-alkyl C (C–OH) (Fig. 4a). The number

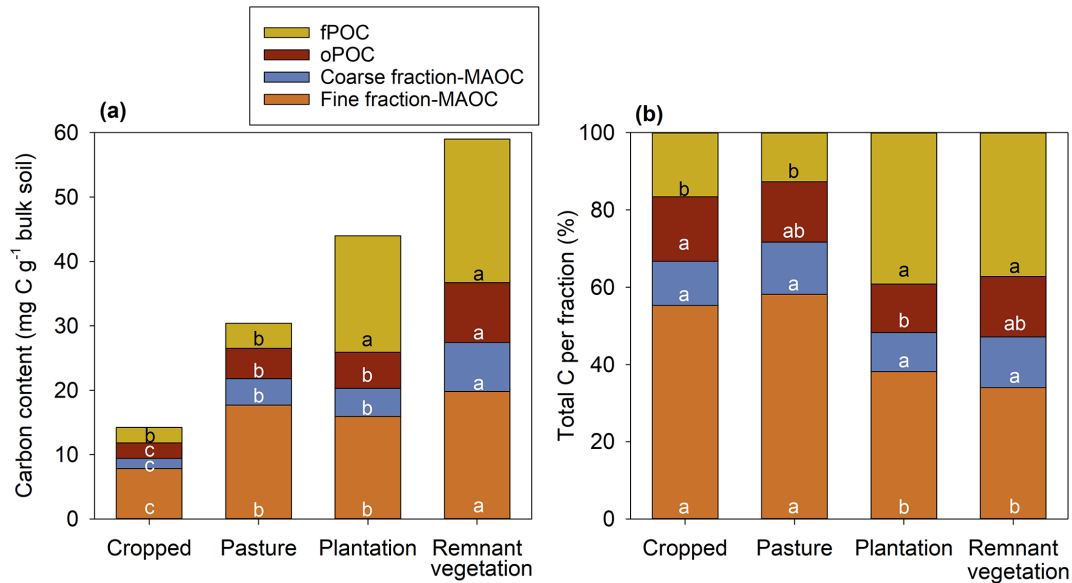


Figure 3. Organic carbon content (a) and the total organic C per fraction (b) for each soil fraction within the bulk soil from topsoils (0–10 cm) collected from four land uses. fPOC is free particulate organic carbon, oPOC is aggregate-occluded particulate organic matter, fine-fraction MAOC is coarse-grained (> 53 μm) mineral-associated organic carbon, and coarse-fraction MAOC is fine-grained (> 53 μm) mineral-associated organic carbon. Lower-case letters indicate least significant differences ($P < 0.05$) between the same fractions across land uses according to the REML mixed-effects model and Tukey's post hoc testing.

of organic C forms observed using NEXAFS did not change with land uses. Importantly, however, we observed differences in the intensities of these peaks within various fractions. In remnant vegetation, the most dominant C function group for all fractions was carboxylic C, ranging from 42%–44% in the POM to 47%–48% in the MAOM (Table 2). This was followed by O-alkyl C for all fractions, accounting for 26% across all fractions. Aliphatic C was the next most dominant C functional group for fine MAOC accounted for 18%. This pattern was observed for the rest of the land uses, namely, dominated by carboxylic C followed by O-alkyl C and aliphatic C. The proportion of C functional groups in the fine MAOC was similar across all land uses with 20% for aliphatic C, 47% for carboxylic C, and 26% for O-alkyl C.

In addition, the N K-edge spectra showed defined peaks at 398.8 eV indicating aromatic N in six-membered rings, 401.2 eV indicating amides, and 406 eV indicating alkyl-N functional groups (Fig. 4b). The amide peak was weaker in the cropped soil compared with the other land uses. However, the aromatic N six-membered rings and alkyl-N peaks were similar between all land uses.

3.5 Distribution of C forms: Synchrotron-based IRM

Synchrotron-based IRM analyses were used to investigate the two-dimensional distribution of C forms within the soil on a microscale, with spectral maps showing the forms of C (aliphatic C, aromatic C, and polysaccharide C) and mineral

OH within 200 nm semi-thin sections taken from intact microaggregates (< 250 μm) (Fig. 5).

For the soil from remnant vegetation (Fig. 5a), it was found that the lateral distribution of clay minerals within the microaggregates correlated strongly with the distribution of aliphatic C ($R^2 = 0.96$), aromatic C ($R^2 = 0.84$), and polysaccharide C ($R^2 = 0.78$). It was observed that aliphatic C in the pasture soil was also correlated with clay minerals ($R^2 = 0.58$) although correlations between aromatic C and clay minerals, as well as between polysaccharide C with clay minerals, were weaker in this soil (Fig. 5b). Similarly, for the plantation soil, there were strong correlations between clay minerals and both polysaccharide C and aliphatic C, whilst aromatic C was only weakly correlated with clay minerals (Fig. 5c). In a similar manner, for the cropped soil (Fig. 5d), strong correlations were found between the distribution of clay minerals and both aliphatic C ($R^2 = 0.92$) and aromatic C ($R^2 = 0.73$), but there was no clear correlation between the distribution of polysaccharide C and clay minerals ($R^2 = 0.24$). The gradients for the regressions of aliphatic C and aromatic C with clay minerals were only marginally lower in the cropped soil than the remnant vegetation. Additionally, for polysaccharide C, the degree of association with clay minerals and the gradient decreased in the following order: remnant vegetation soil > plantation soil > pasture soil > cropped soil.

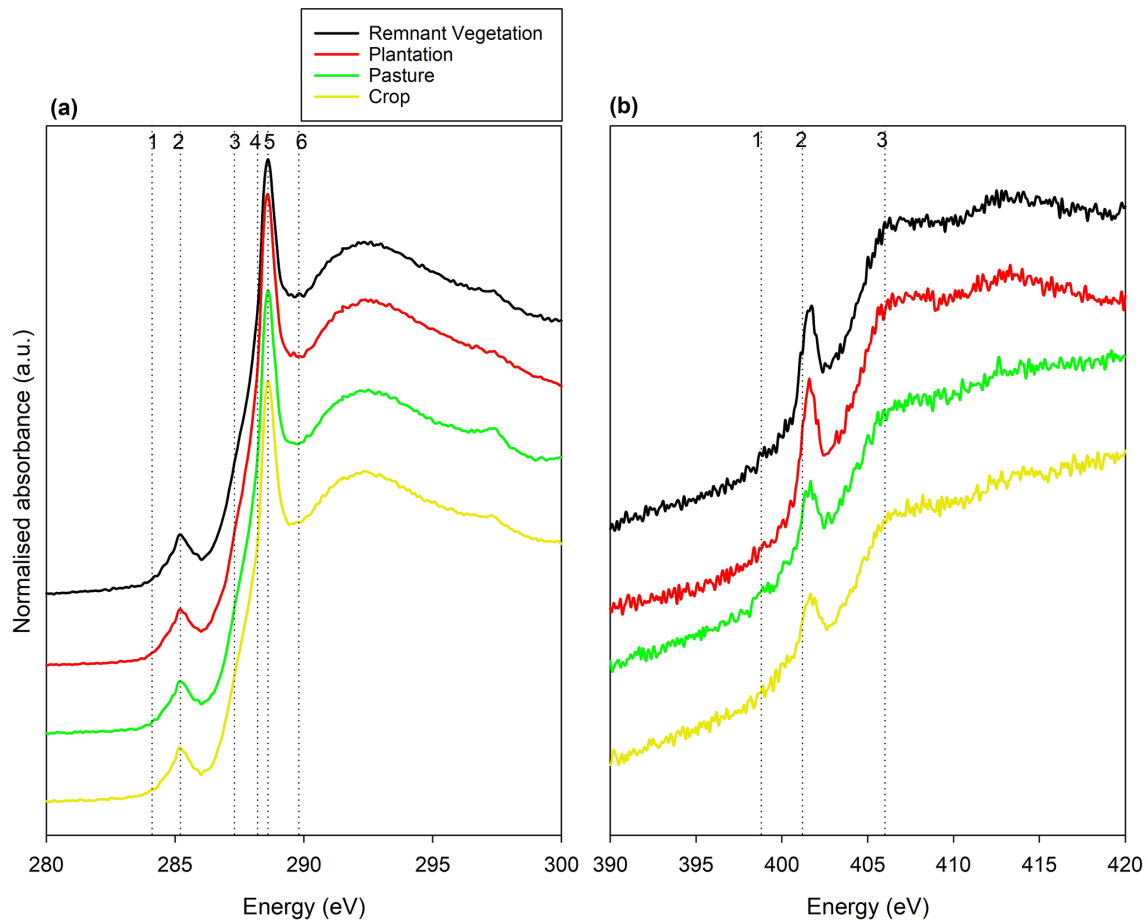


Figure 4. Double-normalized (a) C K-edge spectra and (b) N K-edge spectra of finely ground bulk soil samples from each land use produced by near-edge X-ray absorption fine structure. Spectra have been stretched in the y direction to visualize each land use. (a) Vertical lines indicate (1) quinones at 284.7 eV, (2) aromatic C at 285.5 eV, (3) aliphatic C at 287.3 eV, (4) phenolic C–OH at 288.2 eV, (5) carboxyl C–OOH at 289.0 eV, and (6) O-alkyl C at 289.8 eV. (b) Vertical lines indicate (1) aromatic N in six-membered rings at 398.8 eV, (2) amide at 401.2 eV, and (3) alkyl-N at 406 eV.

4 Discussion

4.1 Land use change to cropping profoundly decreases SOC and N contents, but partial protection is provided by occlusion or binding to the mineral fraction

In this semi-arid subtropical Ferralsol, conversion of remnant vegetation to long-term cropping resulted in the loss of 78 % of total SOC at a depth of 0–10 cm after 72 years (Table 1). Globally, long-term cropping has been identified to reduce SOC stocks by 20 %–60 % (Kopittke et al., 2017). The high loss of C in the cropped soil in the present study could possibly be attributed to the warm, subtropical climate compared to other studies conducted on soils of temperate regions. In addition, Ferralsols have been found to lose a greater proportion of surface-layer SOC than other soil types (Hartemink, 1997), which may explain the very high C loss observed in the present cropped soil. In addition to changes in SOC

contents caused by land use conversion to cropped land, it was observed that there was a 74 % decrease in total N, with decreases also reported in previous studies under long-term cropping (Dalal et al., 2021b; Kopittke et al., 2017).

Not only did land use change cause marked changes in total SOC and N contents, but it was also found that there were substantial changes in the various SOC and N fractions within the soil. Overall, it was observed that the fine-fraction MAOM made the largest contribution to the total SOC and N contents regardless of land use (Figs. 3a and S5). These findings regarding the importance of the fine-fraction MAOC are consistent with previous studies, even following land management changes (Degryze et al., 2004; John et al., 2005; Kleber et al., 2015). In addition, MAOM has been identified to be one of the largest N pools and total N has been shown to be highly correlated with C for the MAOM fraction for a variety of soils (Kirkby et al., 2011).

Table 2. Relative proportion of organic C functional groups in the various fractions under different land uses identified by C (1 s) near-edge X-ray absorption fine-structure (NEXAFS) spectroscopy. fPOC is free particulate organic carbon, oPOC is aggregate-occluded particulate organic matter, coarse-fraction MAOC is coarse-grained (> 53 µm) mineral-associated organic carbon, and fine-fraction MAOC is fine-grained (< 53 µm) mineral-associated organic carbon. Quinones (C=O) at 284.7 eV, aromatic C at 285.5 eV, aliphatic C at 287.3 eV, double-bonded alkyl C (C=C) and phenolic C–OH at 288.2 eV, carboxyl C–OOH at 289.0 eV, and O-alkyl C at 289.8 eV. Statistical significance according to the REML mixed-effects model based on Tukey's post hoc testing (*p* values).

Fractions	Land use	Quinine	Aromatic	Phenolic	Aliphatic	Carboxylic	O-alkyl C
		(%)					
fPOC	Cropped	0.67 ± 0.17	5.3 ± 0.27	4.8 ± 0.46	21 ± 0.27	41 ± 0.87	26 ± 0.25
	Pasture	0.79 ± 0.31	5.3 ± 0.41	4.2 ± 0.35	22 ± 0.23	41 ± 0.68	26 ± 0.36
	Plantation	0.29 ± 0.07	5.9 ± 0.79	3.3 ± 0.56	25 ± 0.43	40 ± 1.8	26 ± 0.15
	Remnant vegetation	0.06 ± 0.02	5.3 ± 0.07	5.3 ± 0.28	20 ± 0.13	44 ± 0.36	26 ± 0.13
oPOC	Cropped	0.10 ± 0.03	5.8 ± 0.13	4.4 ± 0.13	19 ± 0.17	42 ± 0.21	28 ± 0.20
	Pasture	0.24 ± 0.07	6.2 ± 0.33	4.3 ± 0.35	21 ± 0.32	41 ± 0.70	27 ± 0.24
	Plantation	0.17 ± 0.06	6.4 ± 0.63	3.9 ± 0.43	23 ± 0.22	40 ± 1.0	27 ± 0.19
	Remnant vegetation	0.07 ± 0.03	5.9 ± 0.53	5.3 ± 0.61	19 ± 0.14	42 ± 1.2	27 ± 0.14
Coarse MAOC	Cropped	0.09 ± 0.04	3.9 ± 0.37	2.7 ± 0.36	20 ± 0.16	47 ± 0.78	26 ± 0.07
	Pasture	0.11 ± 0.03	4.1 ± 0.51	2.9 ± 0.53	19 ± 0.12	48 ± 0.94	26 ± 0.11
	Plantation	0.07 ± 0.02	4.1 ± 0.46	2.8 ± 0.47	20 ± 0.18	48 ± 1.0	26 ± 0.13
	Remnant vegetation	0.14 ± 0.02	3.4 ± 0.46	2.4 ± 0.52	20 ± 0.07	48 ± 0.96	26 ± 0.12
Fine MAOC	Cropped	0.08 ± 0.03	3.7 ± 0.32	2.5 ± 0.28	19 ± 0.03	48 ± 0.52	26 ± 0.07
	Pasture	0.18 ± 0.04	4.7 ± 0.71	3.1 ± 0.61	20 ± 0.55	47 ± 1.2	25 ± 0.47
	Plantation	0.19 ± 0.03	3.2 ± 0.31	1.8 ± 0.30	20 ± 0.41	49 ± 0.54	26 ± 0.33
	Remnant vegetation	0.12 ± 0.04	4.7 ± 0.31	3.6 ± 0.26	18 ± 0.38	47 ± 0.74	26 ± 0.14
Statistical significance	fPOC	0.057	0.777	0.044	< 0.001	0.116	0.065
	oPOC	0.147	0.798	0.081	< 0.001	0.211	0.002
	Coarse MAOC	0.242	0.731	0.905	< 0.001	0.884	0.451
	Fine MAOC	0.19	0.159	0.067	0.061	0.341	0.105

Although the fine-fraction MAOC was the dominant fraction, it was found that conversion of remnant vegetation to cropped land caused the loss of C and N from all fractions (i.e. decreased their absolute size, Figs. 3a and S5), with this being consistent with previous studies for both organic C (Degryze et al., 2004; John et al., 2005; Six et al., 1998) and N (Yang et al., 2022). Although the size of all fractions decreased for both organic C and N, it was noted that the magnitude of the decrease was greatest for the fPOC fraction and least for the fine-fraction MAOC (Fig. 3a). Indeed, the fPOC fraction accounted for 37 % of the total SOC in the remnant vegetation but only 17 % in the cropped soil, while the fine-fraction MAOC accounted for 34 % of the total SOC in the remnant vegetation but 55 % in the cropped soil (Fig. 3b). This observation that the fPOC fraction is the most susceptible to loss upon conversion to long-term cropping for a subtropical soil is consistent with previous studies from temperate (Six et al., 1998; Besnard et al., 1996) and tropical regions (Ashagrie et al., 2007). This marked loss of fPOM upon land use change to long-term cropping is critical, given that this is the most labile fraction and hence plays an integral role in nutrient cycling and soil biological prop-

erties due to its nature as an easily accessible substrate for microorganisms.

It is also noteworthy that although fPOM was the most labile fraction, the occlusion of the POM within soil aggregates (i.e. oPOM) was important for its resilience – whilst the relative contribution of fPOM significantly decreased from 37 % to 17 % upon conversion to long-term cropping, oPOM remained relatively constant (15.6 % to 16.7 %, Fig. 3b). Thus, these data highlight not only the importance of the binding of SOC to the mineral fraction (MAOC) but also the importance of soil structure to enable the occlusion of POM (oPOM) in increasing resilience and stability of SOC in subtropical, semi-arid soils.

4.2 The marked loss of labile SOC resulted in decreased microbial activity

The loss of 78 % of the SOC in this subtropical soil at 0–10 cm depth upon conversion to long-term cropping (Table 1), coupled with the preferential loss of the fPOM fraction (Fig. 3a), resulted in a significant decrease in microbial functioning as measured using the microbial respiration rate. Indeed, it was observed that respiration was significantly

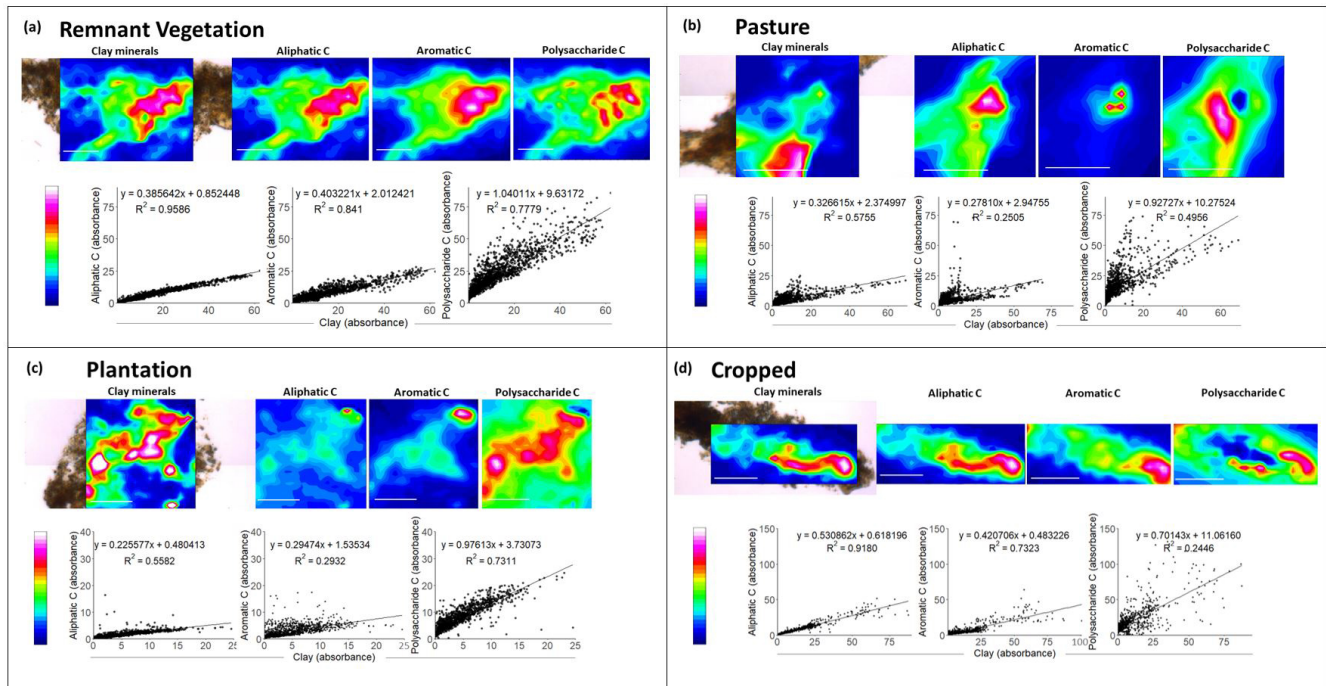


Figure 5. Spectral maps showing the distribution of mineral OH, aliphatic C, aromatic C, and polysaccharide C obtained through Synchrotron-based infrared microspectroscopy by analysis of sections (200 nm thickness) obtained from intact microaggregates of soil from four land uses (remnant vegetation, pasture, plantation, and cropped) (bars are 25 μm). The spectral map of one of the two to three replicates analysed for each land use is shown. Maps were obtained from 32 co-added scans (4 cm^{-1} resolution) with a 2.5 μm step size. The spectra obtained from each map were used to form regression analyses. Pixels where the absorption peak could not be detected above the baseline noise were excluded from regressions.

lower in the cropped soil than for all other land uses (Fig. 2a). Reduced respiration in surface soils has been shown to be associated with lower SOC levels given that SOC is the substrate for soil microorganisms (Fan et al., 2015; Wang et al., 2013). Thus, the loss of 78 % of the SOC upon conversion to cropped land not only increases CO_2 emissions to the atmosphere (as a greenhouse gas), but the loss of SOC also adversely impacts the functioning of soil, as shown through decreases in microbial respiration.

It must also be noted that it cannot be excluded that the decrease observed in microbial respiration rate in the cropping system could potentially, to some extent, be associated with the application of pesticides. In this regard, pesticides have been reported to adversely affect the soil microbial community, although there are conflicting reports in this regard, and their effects remain unclear (Hussain et al., 2009).

4.3 Changing land use from cropping back to pasture or plantation can partially restore SOC and microbial activity

Whilst conversion of remnant vegetation to cropped land resulted in the loss of 78 % of the SOC, this could be reversed, although not fully, by conversion of cropped soil to pasture or plantation. Indeed, although not significantly different,

conversion of the cropped land to pasture increased the total SOC content by 111 %, whilst conversion of cropped to pasture and then to plantation increased SOC by 250 % (Table 1). Importantly, SOC remained lower in the pasture soil (38 g kg^{-1}) than in the remnant vegetation (81 g kg^{-1}), but in the plantation soil (63 g kg^{-1}), the SOC was increased to a level that was not significantly lower than the remnant vegetation (Table 1). Furthermore, conversion of the cropped soil to pasture significantly increased the total N content by 94 % (Table 1).

This increase in both organic C and N when cropped soil was converted to pasture was associated with increases in all fractions with the exception of fPOM (i.e. increases in oPOM, fine-fraction MAOM, and coarse-fraction MAOM) (Figs. 3a and S5). Of these, the largest absolute increase was for the fine-fraction MAOC, which increased from 7.8 mg g^{-1} of bulk soil in the cropped soil to 18 mg g^{-1} of bulk soil in the pasture. This increase in organic C and N content of the fine-fraction MAOM upon conversion of cropped land to pasture in the present study is likely due to the higher below- and above-ground input of soil organic matter (SOM) in grasslands and lower-intensity disturbance in grasslands. In addition, Ferralsols are rich in iron oxides which can act as an integral regulator for MAOM formation and can lead to rapid accrual of MAOC (Kleber et al., 2015;

Ye et al., 2019). This observed pattern of restoration of the SOC pools upon conversion to pasture is interesting in the context of the soil continuum model proposed by Lehmann and Kleber (2015). It is thought that the increase in biomass input that occurs with the transition from cropping to pasture would first regenerate the fPOM pool, but presumably this pool continued to be rapidly converted to oPOM and ultimately mineral-associated forms. Perhaps this fPOM pool has not yet been restored in the pasture soil as a result of the relatively low rate of biomass production in this environment or the fast turnover of POM within this subtropical climate.

Not only did conversion from cropped land to pasture generally increase SOC in the various fractions, but conversion to plantation also resulted in a significant increase in the C and N content of all fractions (Figs. 3a and S5). Interestingly, the largest increase in organic C and N for the plantation soil was observed for the fPOM fraction, with fPOC and fPON both increasing by more than 656 % (Figs. 3a and S5). Therefore, the restoration of the labile fPOM pool with conversion of cropped land to plantation was a key component of the increase in total SOC seen with this change (Table 1). This increase in the C content of the majority of fractions due to the conversion of cropped land to pasture and plantation, including a large increase in labile fPOC from conversion to plantation, resulted in an increase in soil respiration (Fig. 2b) and thus the restoration of microbial activity. However, although the plantation soil was able to restore the total C to a level not significantly less than remnant vegetation (Table 1), the organic C content of the MAOC fractions and oPOC, still remained significantly lower in the plantation soil compared to the remnant vegetation (Fig. 3a).

This study illustrates the difficulty in restoring C as part of GHG removal (i.e. negative emission technologies, NETs) within semi-arid landscapes of subtropical regions, even in situations where productive land is removed from agriculture and returned to plantation. Indeed, even 39 years after converting cropped soil to pasture, SOC contents remained markedly lower in pasture (38 g kg^{-1}) than remnant vegetation (81 g kg^{-1}). Conversion of cropped land to plantation (63 g kg^{-1}) did restore total SOC contents to a level not significantly less than the remnant vegetation, but most C fractions remained significantly lower. Given that large-scale deployment of NETs is required to keep warming below 1.5°C , this will represent a substantial challenge whilst also continuing to increase food production from soil (Kopittke et al., 2019).

4.4 Speciation and distribution of organic C associated with land use conversion

Despite the significant loss in total SOC, fPOC, and MAOC with long-term cropping, there was no noticeable shift in C functional groups in bulk soils across any of the land uses (Fig. 4a). The C K-edge spectra indicated that quinones, aliphatic C and phenolic C–OH, aromatic C, and carboxyl

C–OOH were present within all land uses. Previous studies have concluded that bulk soils which differed in climate, vegetation compositions, and mineralogy (Lehmann et al., 2008; Solomon et al., 2005) or organic matter at different stages of degradation (Solomon et al., 2007) have markedly similar C forms. This is confirmed by estimating the proportion of C functional groups using deconvolution of NEXAFS peaks in the present study (Table 2). The proportion of C functional groups was similar for all SOC fractions across land uses, indicating the SOC persistence was not a result of the presence of complex C structures but rather a collection of simple and similar C functional composition.

For the N K-edge spectra, all land uses exhibited peaks likely corresponding to aromatic N in six-membered rings, amide, and alkyl-N (Fig. 4b). However, the amide peak for the cropped soil was weaker than the other land uses, which may suggest that this form of N is being more heavily consumed or mineralized by microbes due to increased soil disturbance in the cropped soil.

Given that there were no pronounced differences when examining bulk soil but notable shifts across various fractions, sections taken from intact microaggregates were examined using Synchrotron-based IRM. It was found that the distribution of C across microaggregate sections was highly heterogeneous (Fig. 5) as has been observed in prior studies (Lehmann et al., 2008; Wan et al., 2007; Weng et al., 2024). It was noted that there was no clear gradient of SOC from the surface to the core of the microaggregates. This agrees with previous studies which examined the SOC distribution of microaggregates using similar methods (Hernandez-Soriano et al., 2018; Weng et al., 2022) and using nanoscale secondary ion mass spectrometry (Kopittke et al., 2018; Steffens et al., 2017). Thus, this evidence does not support the hypothesis that microaggregates are formed by mineral particles encapsulating organic fragments (Six et al., 1998; Tisdall and Oades, 1982).

It was also noteworthy that there were clear correlations between the various forms of C and clay minerals regardless of land use, which would suggest that mineral associations are an integral mechanism which stabilizes these C forms (Fig. 5). This observation from in situ IRM analyses from the intact microaggregates supports observations from the fractionation analysis, which demonstrated that the binding of C to the mineral fraction (i.e. the MAOC) is critical in determining SOC persistence, even in long-term cropped soil (Fig. 3). This study is the first to utilize in situ IRM analyses on the fine scale to confirm fractionation findings regarding the importance of MAOC in C persistence. This information is critical in developing mechanistic models to enable better predictions of SOC persistence and the effects of land use change on SOC concentrations for climate change mitigation (Lehmann et al., 2020b).

Not only did the in situ IRM analyses confirm the importance of clay minerals in the binding and protection of SOC, but also differences were observed in the distributions

of forms of C within the sections. More specifically, the correlation between aliphatic C and clay minerals was strong in both the remnant vegetation and the cropped soil. This indicates that aliphatic C remained strongly associated with clay minerals under cropping, which goes against past findings that suggest long-term cropping reduces mineral associations with aliphatic C (Hernandez-Soriano et al., 2018). Considering that aliphatic C (wax layers on roots and leaves of terrestrial higher plants and metabolites and sugars from microbial debris; Jansen et al., 2010) is selectively stabilized by iron oxides (Adhikari and Yang, 2015), which are abundant in Ferralsols, and that fine-fraction MAOC was proportionally the largest C pool for the cropped soil (Fig. 3b), it is likely that mineral-associated aliphatic C is one of the remaining persistent C forms in the cropped soil. This hypothesis is supported by the significant reduction in soil respiration for the cropped soil compared with the other land uses (Fig. 2). This suggests that there are few easily degradable forms of C remaining in the cropped soil and only persistent (not easily degraded) forms of C, such as persistent aliphatic C moieties, have remained in strong association with clay minerals.

Mineral-associations with polysaccharide C decreased in the order of remnant vegetation soil > plantation soil > pasture soil > cropped soil (Fig. 5). Polysaccharide C is often a more easily degradable C form than aliphatic C, and polysaccharide C was found to have a decreased degree of association with minerals with long-term cropping in several previous studies (Hernandez-Soriano et al., 2016; Solomon et al., 2007, 2005). In addition, Solomon et al. (2005) found that polysaccharide C was reduced in the order of natural forests > plantations > cropping, as was observed here, likely due to accelerated mineralization with cropping, as well as lower biomass input under cropping.

4.5 Study limitations

Given that these five samples collected at random points within a single treatment unit, they are considered to be pseudoreplicates (Hurlbert, 1984). No information was available for the sites and their properties from prior to land use change (i.e. 72 years prior), and nor was any information available for the sites when they were converted from cropping to pasture or from pasture to plantation. Rather, the present study uses the space-for-time substitution approach as an alternative to long-term studies and has been regularly used for examining the effects of land disturbance (Pickett, 1989). One of the main issues associated with the space-for-time substitution approach is that there may be underlying spatial variability that is not accounted for and which can alter findings (Pickett, 1989). In this regard, the use of mixed-effects models allows us to compare the variance within the plots to the variance of the treatments with confidence.

We also note that it has been reported for subtropical soils of Queensland (Australia) that climate change is resulting in an overall slight increase in SOC over time (Dalal et al.,

2021a), and although climate change would impact all land uses in the present study, the effects on increased biomass production were likely more pronounced for the remnant vegetation treatment than for the other land uses.

Finally, it is also noted that the cropped soils have had fertilizer applied, whilst no fertilizers have been applied to the pasture or plantation soils (Table S1). In this regard, the application of the low rates of fertilizer to the cropping soil would have impacted upon plant growth and the C and N in these soils. Indeed, it is known that application of fertilizers can alter concentrations of SOC, including in soils of Queensland (Australia) (Jha et al., 2022). Regardless, given that fertilization is part of typical management of these cropping soils and that the aim of this study was to examine the effect of land use change and management (including cropping) on SOC, this is not considered to be a problem.

5 Conclusions

This study has shown that long-term use of a subtropical Ferralsol in Australia for cropping resulted in the loss of > 70 % of both organic C and N compared with remnant vegetation. The organic C that was bound in the mineral fraction of the soil (i.e. the fine-fraction MAOC) was the most protected, whilst the fPOC fraction was the most susceptible to loss and had the lowest concentration in the cropped soil. Due to this loss of organic C, and especially the preferential loss of labile organic C, this research showed that microbial activity was greatly reduced in the cropped soil, with this having important implications for soil fertility and functioning. Not only did fractionation demonstrate the importance of the binding of C to the mineral fraction in regulating C persistence, but *in situ* analyses also confirmed the strong binding of organic C to clay minerals, even in soil used for cropping for 72 years. Interestingly, despite the profound loss of organic C and N upon long-term cropping, NEXAFS analyses demonstrated that the forms of organic C within bulk soils were actually similar across all land uses. However, aliphatic C was enriched in the fine MAOC fraction (< 53 μm) regardless of land uses, indicating the role of microbial processing in organo-mineral interactions. Furthermore, the enrichment of carboxylic C in the fPOC fraction in the cropped soil suggested the vulnerability of SOC to be decomposed after long-term cropping. Finally, it was also examined whether conversion of this subtropical Ferralsol used for cropping to either pasture or plantation could restore the lost organic C and N. It was observed that although C and N contents increased after cropping, with increases in all fractions (especially the more labile fPOM fraction), even after up to 39 years, C content within all fractions had not been restored to those observed in the remnant vegetation soil. These data show that whilst soil can be used as a NET to mitigate climate change, even when soil is removed from productive agriculture, sequestering C and restoring it to the pre-management levels is dif-

ficult, especially when humans are actually demanding that global food production from soil must be increased.

Code and data availability. The data and analyses that support these findings will be made available in response to a reasonable request but are not hosted in an online repository at this time in order to protect the privacy of growers.

Supplement. The supplement related to this article is available online at: <https://doi.org/10.5194/soil-10-451-2024-supplement>.

Author contributions. PMK, RCD, and ZHW designed the experiments, and LH and MB carried them out. LH drafted the manuscript with contributions from all authors.

Competing interests. The contact author has declared that none of the authors has any competing interests.

Disclaimer. Publisher's note: Copernicus Publications remains neutral with regard to jurisdictional claims made in the text, published maps, institutional affiliations, or any other geographical representation in this paper. While Copernicus Publications makes every effort to include appropriate place names, the final responsibility lies with the authors.

Acknowledgements. We thank the beamline scientists at the Australian Synchrotron, Bruce Cowie and Lars Thomsen, for their technical support of the NEXAFS analysis and Mark Tobin, Annaleise Klein, and Jitraporn (Pimm) Vongsvivut for their technical support of the IRM analysis.

Financial support. This research has been supported by the Grains Research and Development Corporation (GRDC) (grant UOQ1910-003RTX). Part of this research was undertaken on the soft X-ray spectroscopy (SXR) beamline and the infrared microspectroscopy (IRM) beamline at the Australian Synchrotron, part of ANSTO (grant nos. AS222_SXR_18487 and AS222_IRM_18449).

Review statement. This paper was edited by Axel Don and reviewed by two anonymous referees.

References

Adhikari, D. and Yang, Y.: Selective stabilization of aliphatic organic carbon by iron oxide, *Scientific Reports*, 5, 11214, <https://doi.org/10.1038/srep11214>, 2015.

Angst, G., Mueller, K. E., Nierop, K. G. J., and Simpson, M. J.: Plant- or microbial-derived? A review on the molecular compo-

sition of stabilized soil organic matter, *Soil Biol. Biochem.*, 156, 108189, <https://doi.org/10.1016/j.soilbio.2021.108189>, 2021.

Asano, M. and Wagai, R.: Evidence of aggregate hierarchy at micro- to submicron scales in an allophanic Andisol, *Geoderma*, 216, 62–74, <https://doi.org/10.1016/j.geoderma.2013.10.005>, 2014.

Ashagrie, Y., Zech, W., Guggenberger, G., and Mamo, T.: Soil aggregation, and total and particulate organic matter following conversion of native forests to continuous cultivation in Ethiopia, *Soil Till. Res.*, 94, 101–108, <https://doi.org/10.1016/j.still.2006.07.005>, 2007.

Besnard, E., Chenu, C., Balesdent, J., Puget, P., and Arrouays, D.: Fate of particulate organic matter in soil aggregates during cultivation, *Eur. J. Soil Sci.*, 47, 495–503, <https://doi.org/10.1111/j.1365-2389.1996.tb01849.x>, 1996.

Dalal, R. C., Thornton, C. M., Allen, D. E., and Kopitke, P. M.: A study over 33 years shows that carbon and nitrogen stocks in a subtropical soil are increasing under native vegetation in a changing climate, *Sci. Total Environ.*, 772, 145019, <https://doi.org/10.1016/j.scitotenv.2021.145019>, 2021a.

Dalal, R. C., Thornton, C. M., Allen, D. E., Owens, J. S., and Kopitke, P. M.: Long-term land use change in Australia from native forest decreases all fractions of soil organic carbon, including resistant organic carbon, for cropping but not sown pasture, *Agr. Ecosyst. Environ.*, 311, 107326, <https://doi.org/10.1016/j.agee.2021.107326>, 2021b.

DeGryze, S., Six, J., Paustian, K., Morris, S. J., Paul, E. A., and Merckx, R.: Soil organic carbon pool changes following land-use conversions, *Glob. Change Biol.*, 10, 1120–1132, <https://doi.org/10.1111/j.1529-8817.2003.00786.x>, 2004.

Fan, L.-C., Yang, M.-Z., and Han, W.-Y.: Soil respiration under different land uses in eastern China, *PLOS ONE*, 10, e0124198, <https://doi.org/10.1371/journal.pone.0124198>, 2015.

Fang, Y., Tavakkoli, E., Weng, Z., Collins, D., Harvey, D., Karimian, N., Luo, Y., Mehra, P., Rose, M. T., Wilhelm, N., and Van Zwieten, L.: Disentangling carbon stabilization in a Calcisol subsoil amended with iron oxyhydroxides: a dual-¹³C isotope approach, *Soil Biol. Biochem.*, 170, 108711, <https://doi.org/10.1016/j.soilbio.2022.108711>, 2022.

Friedlingstein, P., Jones, M. W., O'Sullivan, M., Andrew, R. M., Bakker, D. C. E., Hauck, J., Le Quéré, C., Peters, G. P., Peters, W., Pongratz, J., Sitch, S., Canadell, J. G., Ciais, P., Jackson, R. B., Alin, S. R., Anthoni, P., Bates, N. R., Becker, M., Belloin, N., Bopp, L., Chau, T. T. T., Chevallier, F., Chini, L. P., Cronin, M., Currie, K. I., Decharme, B., Djutouchouang, L. M., Dou, X., Evans, W., Feely, R. A., Feng, L., Gasser, T., Gilfillan, D., Gkritzalis, T., Grassi, G., Gregor, L., Gruber, N., Gürses, Ö., Harris, I., Houghton, R. A., Hurtt, G. C., Iida, Y., Ilyina, T., Luijkx, I. T., Jain, A., Jones, S. D., Kato, E., Kennedy, D., Klein Goldewijk, K., Knauer, J., Korsbakken, J. I., Körtzinger, A., Landschützer, P., Lauvset, S. K., Lefèvre, N., Lienert, S., Liu, J., Marland, G., McGuire, P. C., Melton, J. R., Munro, D. R., Nabel, J. E. M. S., Nakaoka, S.-I., Niwa, Y., Ono, T., Pierrot, D., Poulter, B., Rehder, G., Resplandy, L., Robertson, E., Rödenbeck, C., Rosan, T. M., Schwinger, J., Schwinghackl, C., Séférian, R., Sutton, A. J., Sweeney, C., Tanhua, T., Tans, P. P., Tian, H., Tilbrook, B., Tubiello, F., van der Werf, G. R., Vuichard, N., Wada, C., Wanninkhof, R., Watson, A. J., Willis, D., Wiltshire, A. J., Yuan, W., Yue, C., Yue, X., Zaehle, S., and

- Zeng, J.: Global Carbon Budget 2021, *Earth Syst. Sci. Data*, 14, 1917–2005, <https://doi.org/10.5194/essd-14-1917-2022>, 2022.
- Hartemink, A. E.: Soil fertility decline in some Major Soil Groupings under permanent cropping in Tanga region, Tanzania, *Geoderma*, 75, 215–229, [https://doi.org/10.1016/S0016-7061\(96\)00087-0](https://doi.org/10.1016/S0016-7061(96)00087-0), 1997.
- Hernandez-Soriano, M. C., Kerre, B., Kopittke, P. M., Horemans, B., de Vos, D., and Smolders, E.: Biochar affects carbon composition and stability in soil: a combined spectroscopy-microscopy study, *Scientific Reports*, 6, 25127, <https://doi.org/10.1038/srep25127>, 2016.
- Hernandez-Soriano, M. C., Dalal, R. C., Warren, F. J., Wang, P., Green, K., Tobin, M. J., Menzies, N. W., and Kopittke, P. M.: Soil organic carbon stabilization: Mapping carbon speciation from intact microaggregates, *Environ. Sci. Technol.*, 52, 12275–12284, <https://doi.org/10.1021/acs.est.8b03095>, 2018.
- Hurlbert, S. H.: Pseudoreplication and the Design of Ecological Field Experiments, *Ecol. Monogr.*, 54, 187–211, <https://doi.org/10.2307/1942661>, 1984.
- Hussain, S., Siddique, T., Saleem, M., Arshad, M., and Khalid, A.: Chapter 5 Impact of Pesticides on Soil Microbial Diversity, Enzymes, and Biochemical Reactions, in: *Adv. Agron., Academic Press*, 159–200, [https://doi.org/10.1016/S0065-2113\(09\)01005-0](https://doi.org/10.1016/S0065-2113(09)01005-0), 2009.
- Jansen, B., van Loon, E. E., Hooghiemstra, H., and Verstraten, J. M.: Improved reconstruction of palaeoenvironments through unravelling of preserved vegetation biomarker patterns, *Palaeogeogr. Palaeoclimatol.*, 285, 119–130, <https://doi.org/10.1016/j.palaeo.2009.10.029>, 2010.
- Jha, P., Hati, K. M., Dalal, R. C., Dang, Y. P., Kopittke, P. M., McKenna, B. A., and Menzies, N. W.: Effect of 50 years of no-tillage, stubble retention, and nitrogen fertilization on soil respiration, easily extractable glomalin, and nitrogen mineralization, *Agronomy*, 12, 151, <https://doi.org/10.3390/agronomy12010151>, 2022.
- John, B., Yamashita, T., Ludwig, B., and Flessa, H.: Storage of organic carbon in aggregate and density fractions of silty soils under different types of land use, *Geoderma*, 128, 63–79, <https://doi.org/10.1016/j.geoderma.2004.12.013>, 2005.
- Kirkby, C. A., Kirkegaard, J. A., Richardson, A. E., Wade, L. J., Blanchard, C., and Batten, G.: Stable soil organic matter: A comparison of C:N:P:S ratios in Australian and other world soils, *Geoderma*, 163, 197–208, <https://doi.org/10.1016/j.geoderma.2011.04.010>, 2011.
- Kleber, M., Eusterhues, K., Keiluweit, M., Mikutta, C., Mikutta, R., and Nico, P. S.: Mineral-organic associations: Formation, properties, and relevance in soil environments, *Adv. Agron.*, 130, 1–140, <https://doi.org/10.1016/bs.agron.2014.10.005>, 2015.
- Kölbl, A. and Kögel-Knabner, I.: Content and composition of free and occluded particulate organic matter in a differently textured arable Cambisol as revealed by solid-state ¹³C NMR spectroscopy, *J. Plant Nutr. Soil Sc.*, 167, 45–53, <https://doi.org/10.1002/jpln.200321185>, 2004.
- Kopittke, P. M., Dalal, R. C., Finn, D., and Menzies, N. W.: Global changes in soil stocks of carbon, nitrogen, phosphorus, and sulphur as influenced by long-term agricultural production, *Glob. Change Biol.*, 23, 2509–2519, 2017.
- Kopittke, P. M., Hernandez-Soriano, M. C., Dalal, R. C., Finn, D., Menzies, N. W., Hoeschen, C., and Mueller, C. W.: Nitrogen-rich microbial products provide new organo-mineral associations for the stabilization of soil organic matter, *Glob. Change Biol.*, 24, 1762–1770, 2018.
- Kopittke, P. M., Menzies, N. W., Wang, P., McKenna, B. A., and Lombi, E.: Soil and the intensification of agriculture for global food security, *Environ. Int.*, 132, 105078, <https://doi.org/10.1016/j.envint.2019.105078>, 2019.
- Lehmann, J. and Kleber, M.: The contentious nature of soil organic matter, *Nature*, 528, 60–68, <https://doi.org/10.1038/nature16069>, 2015.
- Lehmann, J., Solomon, D., Kinyangi, J., Dathe, L., Wirrick, S., and Jacobsen, C.: Spatial complexity of soil organic matter forms at nanometre scales, *Nat. Geosci.*, 1, 238–242, 2008.
- Lehmann, J., Bossio, D. A., Kögel-Knabner, I., and Rillig, M. C.: The concept and future prospects of soil health, *Nature Reviews Earth & Environment*, 1, 544–553, <https://doi.org/10.1038/s43017-020-0080-8>, 2020a.
- Lehmann, J., Hansel, C. M., Kaiser, C., Kleber, M., Maher, K., Manzoni, S., Nunan, N., Reichstein, M., Schimel, J. P., Torn, M. S., Wieder, W. R., and Kögel-Knabner, I.: Persistence of soil organic carbon caused by functional complexity, *Nat. Geosci.*, 13, 529–534, <https://doi.org/10.1038/s41561-020-0612-3>, 2020b.
- Niaz, S., Wehr, J. B., Dalal, R. C., Kopittke, P. M., and Menzies, N. W.: Organic amendments and gypsum reduce dispersion and increase aggregation of two sodic Vertisols, *Geoderma*, 425, 116047, <https://doi.org/10.1016/j.geoderma.2022.116047>, 2022.
- Oldfield, E. E., Bradford, M. A., and Wood, S. A.: Global meta-analysis of the relationship between soil organic matter and crop yields, *SOIL*, 5, 15–32, <https://doi.org/10.5194/soil-5-15-2019>, 2019.
- Pickett, S. T. A.: Space-for-Time Substitution as an Alternative to Long-Term Studies, in: *Long-Term Studies in Ecology: Approaches and Alternatives*, edited by: Likens, G. E., Springer New York, New York, NY, 110–135, https://doi.org/10.1007/978-1-4615-7358-6_5, 1989.
- Prietzl, J., Müller, S., Kögel-Knabner, I., Thieme, J., Jaye, C., and Fischer, D.: Comparison of soil organic carbon speciation using C NEXAFS and CPMAS ¹³C NMR spectroscopy, *Sci. Total Environ.*, 628–629, 906–918, <https://doi.org/10.1016/j.scitotenv.2018.02.121>, 2018.
- R Core Team: R: A language and environment for statistical computing. R Foundation for Statistical Computing, Vienna, Austria, <https://www.R-project.org/> (last access: 28 June 2024), 2021.
- Ravel, B. and Newville, M.: Athena, Artemis, Hephaestus: Data analysis for X-ray absorption spectroscopy using IFEFFIT, *J. Synchrot. Radiat.*, 12, 537–541, <https://doi.org/10.1107/S0909049505012719>, 2005.
- Rayment, G. E. and Lyons, D. J.: *Soil Chemical Methods: Australasia*, CSIRO Publishing, Collingwood, Australia, 495 pp., <https://doi.org/10.1071/9780643101364>, 2011.
- Sanderman, J., Hengl, T., and Fiske, G. J.: Soil carbon debt of 12000 years of human land use, *P. Natl. Acad. Sci. USA*, 114, 9575–9580, <https://doi.org/10.1073/pnas.1706103114>, 2017.
- Six, J., Elliott, E. T., Paustian, K., and Doran, J. W.: Aggregation and soil organic matter accumulation in cultivated and native grassland soils, *Soil Sci. Soc. Am. J.*, 62, 1367–1377, <https://doi.org/10.2136/sssaj1998.03615995006200050032x>, 1998.

- Solomon, D., Lehmann, J., Kinyangi, J., Liang, B., and Schäfer, T.: Carbon K-edge NEXAFS and FTIR-ATR spectroscopic investigation of organic carbon speciation in soils, *Soil Sci. Soc. Am. J.*, 69, 107–119, 2005.
- Solomon, D., Lehmann, J., Kinyangi, J., Amelung, W., Lobe, I., Pell, A., Riha, S., Ngoze, S., Verchot, L. O. U., Mbugua, D., Skjemstad, J. A. N., and Schäfer, T.: Long-term impacts of anthropogenic perturbations on dynamics and speciation of organic carbon in tropical forest and subtropical grassland ecosystems, *Glob. Change Biol.*, 13, 511–530, <https://doi.org/10.1111/j.1365-2486.2006.01304.x>, 2007.
- Spielvogel, S., Prielzel, J., and Kögel-Knabner, I.: Changes of lignin phenols and neutral sugars in different soil types of a high-elevation forest ecosystem 25 years after forest dieback, *Soil Biol. Biochem.*, 39, 655–668, <https://doi.org/10.1016/j.soilbio.2006.09.018>, 2007.
- Steffens, M., Kölbl, A., and Kögel-Knabner, I.: Alteration of soil organic matter pools and aggregation in semi-arid steppe topsoils as driven by organic matter input, *Eur. J. Soil Sci.*, 60, 198–212, <https://doi.org/10.1111/j.1365-2389.2008.01104.x>, 2009.
- Steffens, M., Rogge, D. M., Mueller, C. W., Höschen, C., Lugmeier, J., Kölbl, A., and Kögel-Knabner, I.: Identification of distinct functional microstructural domains controlling C storage in soil, *Environ. Sci. Technol.*, 51, 12182–12189, <https://doi.org/10.1021/acs.est.7b03715>, 2017.
- Stöhr, J.: NEXAFS spectroscopy, 25, 159–161, Springer Science & Business Media, ISBN 3662028530, 9783662028537, 2013.
- Sykes, A. J., Macleod, M., Eory, V., Rees, R. M., Payen, F., Myrgiotis, V., Williams, M., Sohi, S., Hillier, J., Moran, D., Manning, D. A. C., Goglio, P., Seghetta, M., Williams, A., Harris, J., Dondini, M., Walton, J., House, J., and Smith, P.: Characterising the biophysical, economic and social impacts of soil carbon sequestration as a greenhouse gas removal technology, *Glob. Change Biol.*, 26, 1085–1108, <https://doi.org/10.1111/gcb.14844>, 2020.
- Tisdall, J. M. and Oades, J. M.: Organic matter and water-stable aggregates in soils, *J. Soil Sci.*, 33, 141–163, <https://doi.org/10.1111/j.1365-2389.1982.tb01755.x>, 1982.
- Wan, J., Tylliszczak, T., and Tokunaga, T. K.: Organic carbon distribution, speciation, and elemental correlations within soil microaggregates: Applications of STXM and NEXAFS spectroscopy, *Geochim. Cosmochim. Ac.*, 71, 5439–5449, <https://doi.org/10.1016/j.gca.2007.07.030>, 2007.
- Wang, W., Zeng, W., Chen, W., Zeng, H., and Fang, J.: Soil respiration and organic carbon dynamics with grassland conversions to woodlands in temperate China, *PLOS ONE*, 8, e71986, <https://doi.org/10.1371/journal.pone.0071986>, 2013.
- Weng, Z., Van Zwieten, L., Singh, B. P., Tavakkoli, E., Joseph, S., Macdonald, L. M., Rose, T. J., Rose, M. T., Kimber, S. W. L., Morris, S., Cozzolino, D., Araujo, J. R., Archanjo, B. S., and Cowie, A.: Biochar built soil carbon over a decade by stabilizing rhizodeposits, *Nat. Clim. Change*, 7, 371–376, <https://doi.org/10.1038/nclimate3276>, 2017.
- Weng, Z., Van Zwieten, L., Tavakkoli, E., Rose, M. T., Singh, B. P., Joseph, S., Macdonald, L. M., Kimber, S., Morris, S., Rose, T. J., Archanjo, B. S., Tang, C., Franks, A. E., Diao, H., Schweizer, S. A., Tobin, M. J., Klein, A. R., Vongsivut, K., Chang, S. L. Y., Kopittke, P. M., and Cowie, A.: Microspectroscopic visualization of how biochar lifts the soil organic carbon ceiling, *Nat. Commun.*, 13, 5177, <https://doi.org/10.1038/s41467-022-32819-7>, 2022.
- Weng, Z. H., Kopittke, P. M., Schweizer, S., Jin, J., Armstrong, R., Rose, M., Zheng, Y., Franks, A., and Tang, C.: Shining a Light on How Soil Organic Carbon Behaves at Fine Scales under Long-Term Elevated CO₂: An 8 Year Free-Air Carbon Dioxide Enrichment Study, *Environ. Sci. Technol.*, 20, 8724–8735, <https://doi.org/10.1021/acs.est.3c10680>, 2024.
- Yang, L., Liu, W., Jia, Z., Li, P., Wu, Y., Chen, Y., Liu, C., Chang, P., and Liu, L.: Land-use change reduces soil nitrogen retention of both particulate and mineral-associated organic matter in a temperate grassland, *Catena*, 216, 106432, <https://doi.org/10.1016/j.catena.2022.106432>, 2022.
- Ye, C., Hall, S. J., and Hu, S.: Controls on mineral-associated organic matter formation in a degraded Oxisol, *Geoderma*, 338, 383–392, <https://doi.org/10.1016/j.geoderma.2018.12.011>, 2019.
- Zhang, Y., Bhattacharyya, R., Dalal, R. C., Wang, P., Menzies, N. W., and Kopittke, P. M.: Impact of land use change and soil type on total phosphorus and its fractions in soil aggregates, *Land Degrad. Dev.*, 31, 828–841, <https://doi.org/10.1002/ldr.3501>, 2020.